

LA-UR- 00 - 1153

Approved for public release;
distribution is unlimited.

Title: Interpretation of Experiments and Modeling of Internal Strains in Beryllium Using a Polycrystal Model

Author(s): Carlos Tome, MST-8
Mark R. Daymond, ISIS - England
Mark A.M. Bourke, MST-8

Submitted to: Sixth International Conference on Residual Stresses
July 10-12, 2000
Oxford, UK

Los Alamos

NATIONAL LABORATORY

Los Alamos National Laboratory, an affirmative action/equal opportunity employer, is operated by the University of California for the U.S. Department of Energy under contract W-7405-ENG-36. By acceptance of this article, the publisher recognizes that the U.S. Government retains a nonexclusive, royalty-free license to publish or reproduce the published form of this contribution, or to allow others to do so, for U.S. Government purposes. Los Alamos National Laboratory requests that the publisher identify this article as work performed under the auspices of the U.S. Department of Energy. Los Alamos National Laboratory strongly supports academic freedom and a researcher's right to publish; as an institution, however, the Laboratory does not endorse the viewpoint of a publication or guarantee its technical correctness.

DISCLAIMER

This report was prepared as an account of work sponsored by an agency of the United States Government. Neither the United States Government nor any agency thereof, nor any of their employees, make any warranty, express or implied, or assumes any legal liability or responsibility for the accuracy, completeness, or usefulness of any information, apparatus, product, or process disclosed, or represents that its use would not infringe privately owned rights. Reference herein to any specific commercial product, process, or service by trade name, trademark, manufacturer, or otherwise does not necessarily constitute or imply its endorsement, recommendation, or favoring by the United States Government or any agency thereof. The views and opinions of authors expressed herein do not necessarily state or reflect those of the United States Government or any agency thereof.

DISCLAIMER

Portions of this document may be illegible in electronic image products. Images are produced from the best available original document.

RECEIVED

OCT 26 2000

OSTI

INTERPRETATION OF EXPERIMENTS AND MODELING OF INTERNAL STRAINS IN BERYLLIUM USING A POLYCRYSTAL MODEL

C N Tomé¹, M R Daymond² and M A M Bourke¹

¹ MST Division, Los Alamos National Lab, Los Alamos, NM 87545, USA

² ISIS, Rutherford Appleton Lab, Chilton, Didcot, Oxon OX11 0QX, England

ABSTRACT

The elastic and plastic anisotropy of Be have been examined during a uniaxial compression test, by in-situ monitoring in a pulsed neutron beam. Comparisons between the measured hkil strains and the predictions from an elasto-plastic self-consistent (EPSC) model are made. Agreement is qualitatively correct for most planes in the elasto-plastic regime. Possible mechanisms responsible for the quantitative discrepancies between model and experiment are discussed.

INTRODUCTION

The use of neutron and x-ray diffraction to measure the spacings of atomic lattice planes and interpretation of their variation in terms of strains has been well established [1, 2, 3]. It has also been recognized that the elastic anisotropy of the single crystal results in different directional stiffness depending on the individual diffraction peak which is being monitored. However once plasticity occurs, the ease of slip upon certain planes preferentially unloads certain lattice planes, and hence the response of individual hkil reflections upon a simple uniaxial load is non-linear.

The modelling of polycrystalline plasticity in metals has been aided in the last few years by comparing neutron diffraction measurements of the response of different hkil reflections during uniaxial loading with model predictions. Validation using *in situ* data is inherently more demanding on the model than simply examining the end residual strains produced by deformation, since not only the latter, but also the path dependence has to be reproduced. Previous work has addressed fcc structures such as steel, aluminum or copper [4], and hexagonal zirconium alloys [5-7]. Here we address industrially pure beryllium with aim of identifying the respective contributions of different crystallographic mechanisms to the hkil anisotropies.

EXPERIMENT

The *in situ* loading measurements were carried out at the Lujan Center, Los Alamos National Lab., using a pulsed neutron source. A description of the technique can be found elsewhere [8]. We performed a series of measurements under uniaxial compressive loading, simultaneously recording the stress-strain response of the sample, and the elastic response of individual reflections. The load frame is

designed for use in the neutron beam [9]. The loading axis is horizontal and at 45° to the incident beam, allowing simultaneous measurements of lattice plane spacing parallel and perpendicular to the load in opposing 90° detector banks. The load was applied in 18 steps to a maximum of 380 MPa and about 1.1% deformation. At each measurement the sample was held at constant load for 30 minutes to provide time to collect sufficient neutrons for good statistics on the single peak fits. During the stress hold some room temperature relaxation was observed, although it was only significant above 300 MPa. Single peak fits were carried out on the 0002 & 0004, 10 $\bar{1}$ 0 & 20 $\bar{2}$ 0, 10 $\bar{1}$ 1 & 20 $\bar{2}$ 2, 10 $\bar{1}$ 2, 10 $\bar{1}$ 3, 10 $\bar{1}$ 4, 11 $\bar{2}$ 0, 20 $\bar{2}$ 1 and 11 $\bar{2}$ 2 peaks. A 'zero' point of -5 MPa was chosen to hold the sample in the grips, and all strains of individual hkil reflections are reported relative to the lattice spacings measured at -5MPa, rather than to a 'stress-free' universal lattice parameter. This *modus operandi* ignores the presence of pre-existing residual strains induced by prior thermal or mechanical treatments.

The source of the Be used for the specimen was a hot isostatically pressed plate which was cut by electrical discharge into a cylindrical sample 24mm long with 10mm diameter. The grain size of the Be was ~45µm, and micrographs showed the material was well consolidated and with an uniform grain size distribution. The diffraction measurements indicate a close-to-random texture.

POLYCRYSTAL MODEL

The elasto-plastic self-consistent (EPSC) model used in this paper is described in detail elsewhere [5,7]. Briefly, a population of grains is chosen with orientations and weights appropriate for the texture which is to be modeled. In this case the random texture was represented by 1000 orientations. Each grain is modeled as a spherical elasto-plastic inclusion embedded in a Homogenous Effective Medium (HEM). The elasto-plastic properties of the HEM correspond to the average of all the grains and they must be solved iteratively. Each grain is defined with appropriate elastic and thermal single crystal constants. The active slip and twinning systems are defined through their Critical Resolved Shear Stress (CRSS) and some hardening behavior. In this work we assumed that all systems have an initial CRSS τ_0^S and that they harden linearly according to a law

$$\Delta\tau^S = \theta_0^S \sum_{s'} \Delta\gamma^{s'} \quad (1)$$

Where θ_0^S is a hardening coefficient and $\Delta\gamma^{s'}$ is the plastic shear increment in system s' . In the model the load was applied in strain control in 110 steps, to a total strain of 1.1% consistent with the experiment, while zero lateral stresses were enforced in the compression sample.

For comparison with the diffraction measurements subsets of grains are chosen whose hkil plane normals are oriented as the measured ones. The average of the strain over all the grains in each subset for the diffracting plane can then be calculated. In practice grains with normals within an angular range ($\pm 5^\circ$) of the exact diffraction requirement are used; this compares with the angular range of the detectors, which is $\pm 5.5^\circ$.

RESULTS AND DISCUSSION

In what follows we compare both the macroscopic stress-strain response and the evolution of crystallographic strains predicted by the EPSC model, with the corresponding experimental values. The purpose is to gain a better understanding of the deformation systems. The single crystal elastic constants used in the calculation are: $C_{11}=292.3$, $C_{33}=336.4$, $C_{12}=26.7$, $C_{13}=14.0$ and $C_{44}=162.5$ GPa [10]. The directional Young's moduli are 335.6 and 289.3 GPa in the directions parallel and perpendicular to the c-axis, respectively, and indicate that the elastic properties of Be are not markedly anisotropic. However, Be exhibits an unusually low Poisson modulus ($\nu=0.038$ in the basal plane). The thermal expansion coefficients of Be are: $\alpha_{11}=10.4$ and $\alpha_{33}=13.9 \times 10^{-6} \text{ K}^{-1}$. Their difference is large enough to expect a build-up of non-negligible internal strains when cooling the material from typical fabrication conditions to room temperature.

While the thermo-elastic properties of the individual grain are reasonably well known, the plastic mechanisms are much less clear. Be has an hcp structure, and undergoes slip readily on the basal (0002) plane, and with a higher critical resolved shear stress (CRSS) on the type 1 prism ($10\bar{1}0$) plane [10]. The observed fracture stress is relatively low on the basal plane, although fracture is also observed on the type 2 prism (1120) plane, and twinning fracture on the pyramidal ($10\bar{1}2$) plane [10]. Basal slip can only accommodate shear in the basal plane and, as a consequence, prismatic slip, and/or pyramidal slip, and/or twinning is required in order to give general deformation. Hence, we explored simulations using different combinations of plastic modes with different yield strengths. Here we choose to report only 4 cases that illustrate the effects of different assumptions. The combination of deformation systems, their associated CRSS's and hardening coefficients are condensed in Table I. We regard case 1 as our best fit to the experimental data, and the results of cases 2 to 4 will be discussed using case 1 as a reference.

The results corresponding to case 1 are reported in Fig.1 and will be described here in some detail, in order to illustrate the connection between plastic activity and crystallographic strain evolution. Figure 1a depicts the predicted and measured macroscopic stress-strain response, together with relative activity of the deformation modes used in the simulation. Basal slip is activated first, followed by prism slip and, only after a deformation of about 1.5×10^{-3} , by pyramidal slip (tensile twins were not activated). In case 1 the model captures the initial elastic response, the elasto-plastic transition, and the final hardening slope. Upon unloading, though, the experimental curve exhibits a marked Bauschinger effect, which for the predicted unloading is very small.

The measured (elastic) strains determined from the diffraction peaks are compared with model predictions parallel (Fig.1b) and transverse (Fig.1c) to the load. Here we only report results for the ($10\bar{1}0$) prism planes, the ($10\bar{1}1$) pyramidal and (0002) basal planes during loading. The other planes are not plotted in order not to clutter the graphs. Full symbols represent model predictions and open symbols represent experimental measurements. The latter are affected by an uncertainty of $\pm 50 \times 10^{-6}$.

Table I: Sets of critical stresses τ_0 [MPa] and hardening parameters θ_0 [MPa] used in the simulations discussed in this work.

	case 1	case 2	case 3	case 4
Basal slip $\langle 11\bar{2}0 \rangle (0002)$	60 800	60 800	60 800	60 800
Prism slip $\langle 11\bar{2}0 \rangle (10\bar{1}0)$	120 800	120 800	120 800	120 800
Pyram slip $\langle 11\bar{2}3 \rangle (11\bar{2}2)$	170 2000	300 2000	300 2000	170 2000
Tensile twin $\langle 10\bar{1}\bar{1} \rangle (10\bar{1}2)$	230 2000	160 2000	-	230 2000
Compr twin $\langle 10\bar{1}\bar{2} \rangle (10\bar{1}1)$	-	-	160 2000	-
ΔT	0	0	0	-300 K

The simulated initial response of the various diffraction planes is strictly linear, which indicates macroscopic elastic loading, until at an applied load of around 100 MPa some deviations from linearity become apparent. These features are not particularly clear in the experimental results, given the experimental uncertainty. As plastic shear starts to occur in certain slip systems, some planes are less able to bear increments in load and show, as a consequence, a smaller increase in elastic strain per increment of applied stress than in the elastic region. Stress equilibrium requires other planes to take up this increased load and, as a consequence, to increase their elastic strain. This is particularly clear in Fig.1c above 250 MPa, where the $(10\bar{1}1)$ and the (0002) planes bear relatively less and more load, respectively, than in the elastic regime.

Case 1 captures most of the experimental features, such as the relative position of each reflection and the signs of the residual strains after unloading. However, it fails to reproduce particular details of the strain evolution. In the first place, the initial slopes of the longitudinal experimental strains (Fig.1b) are smaller than the minimum Young modulus of the single crystal. This may be signaling the presence of plastic relaxation from the beginning of the experiment. Also, since the first point is taken as a reference for the subsequent measurements, an inaccuracy associated with the first measurements could be responsible for the shift observed between experiment and model at small stresses. Such shift would also affect the prediction of residual strains upon unloading. As for the transverse strains (Fig.1c), the initial elastic slope is very steep due to the nearly zero Poisson modulus of Be, and the model captures this effect correctly. It also captures the split of the three peaks above a stress of 100 MPa, when basal becomes active, as well as the dramatic changes in slope when pyramidal slip relaxation begins at about 250 MPa. All the above features are present in the experimental measurements, and the sign of the residual strains upon unloading is also correctly reproduced. However, the experiment indicates that the basal and the pyramidal planes eventually carry around twice as much load as the model predicts. We find that changing the parameters of the deformation modes to increase these strains adversely affects the prediction of the longitudinal ones.

The fits represented in Fig.1 are predicated on the activation of pyramidal slip, a deformation mode not reported for Be. As was mentioned above, single crystal Be is known to undergo both fracture of the basal plane and pyramidal twinning, which are not included in the calculation of case 1. Any of these mechanisms would induce strain relaxation in selected crystallographic planes, although including twinning or fracture effects in a polycrystal model is not straightforward. If twinning were active, one effect would be to alter the diffraction peak intensity, increasing certain peak heights, and decreasing others. No experimental evidence for this was found, but this may only be due to the fact that the twinning volume is less than about 5%, below the resolution of the NPD instrument.

To assess the possible twinning implications in the strain evolution, in case 2 we activate tensile twinning of the type $(10\bar{1}2)(10\bar{1}1)$, by lowering the initial CRSS of twinning and increasing that of pyramidal slip (see Fig. 2 and Table I). In our model twinning is treated as a directional plastic shear mechanism which can be activated in only one direction, but no other relaxation effects are accounted for. Although the macroscopic response is still reasonably reproduced (Fig.2a), grains oriented with the c-axis along the compression direction cannot deform by twinning and, as a consequence, they accumulate large elastic strains across the (0002) basal planes until pyramidal slip is enabled and relaxation takes place. Such response is evident in Fig. 2b, where the predicted basal strain grossly exceeds the observed evolution of the (0002) strains. As for the transverse strains (Fig.2c), the twinning activity induces relaxation in grains with the c-axis perpendicular to the compression axis, and forces other orientations to carry more load. As a consequence the predicted evolution of the transverse (0002) and $(10\bar{1}0)$ strains exhibits a larger deviation from the experiment than in case 1. The results of case 2 are puzzling given reported deformation modes, since they may indicate that tensile twinning is not an active mode under the present experimental conditions.

The fact that a directional mechanism may be responsible for the observed evolution of internal strains is illustrated in case 3, where we consider the presence of compressive twinning of the type $(10\bar{1}1)(10\bar{1}2)$. We achieve this by switching the CRSS's of pyramidal slip and twinning (see Table I). The macroscopic response is still reasonably reproduced (Fig.3a) and the twinning activity in grains with the c-axis parallel to the compressive direction does not change the response of the longitudinal strains with respect to case 1 (Fig.3b). A change in the correct direction is observed, however, for the transverse strains (Fig.3c): the share of load in the basal planes increases without the benefit of relaxation from the hard pyramidal slip and, as a consequence the load in the prismatic $(10\bar{1}0)$ planes decreases, giving an evolution more compatible with the one observed experimentally, although achieved by assuming a deformation mode uncharacteristic of Be.

Finally, in case 4 we analyze the effect that initial thermal residual strains may have on the subsequent mechanical response. Using the same plastic parameters as case 1 (Table I), the calculation is preceded by a build up of thermal strains associated with cooling a stress-free aggregate at 325°C down to 25°C. Given the thermal expansion coefficients of Be, the net effect is to induce tensile strains across the basal (0002) planes and compressive strains across the prismatic

planes. During subsequent compression, these pre-existing thermal stresses lower the macroscopic yield stress (Fig.4a) and affect the evolution of internal strains. In particular, the initial tensile stress along the c-axis allows those grains with the c-axis parallel to the compression axis to accumulate more compressive load in the basal planes before pyramidal slip kicks in (Fig.4b). Concurrently, the contribution from these same grains to the $(10\bar{1}0)$ peak in the transverse direction shows that they increase their share of tensile strain, thus relieving the grains with the c-axis perpendicular to the compression axis (i.e. transverse basal peaks, Fig.4c). As a consequence of this strain shift the agreement between model and measurements is worse for the case 4 than for the case 1.

CONCLUSIONS

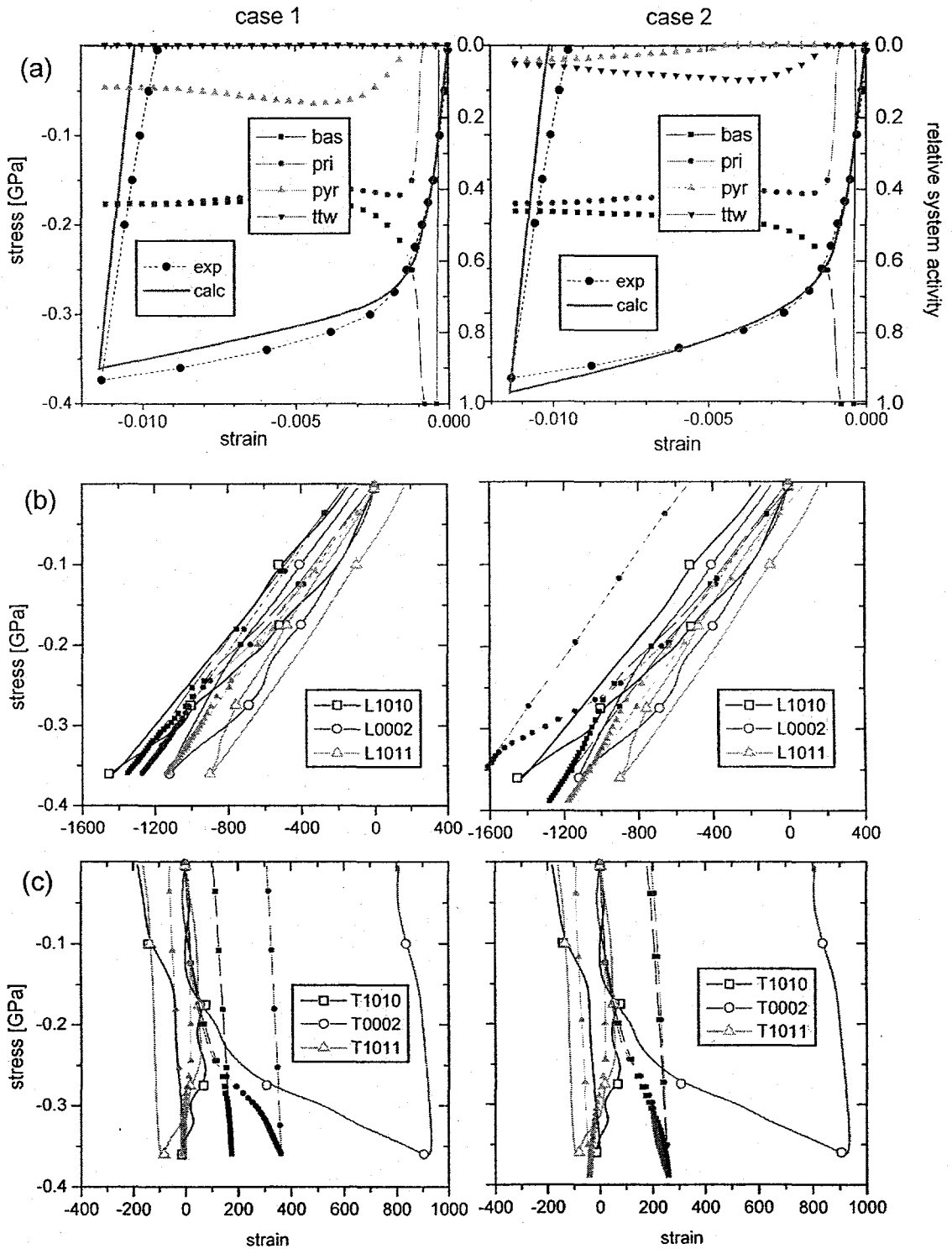
In-situ measurements of the elastic strain response of different diffraction peaks have been carried out for Be under increasing compressive loads, to 1.1% plastic strain. These results are compared with predictions from an EPSC model. Our findings are puzzling in several respects: a) the experimental evidence seems to be compatible with pyramidal slip activity or, to a lesser extent, with compressive twinning, neither of which are reported in Be; b) the inclusion of more obvious mechanisms, such as tensile twinning or thermal residual strains, predict trends which are contrary to the experimental evidence.

ACKNOWLEDGEMENTS

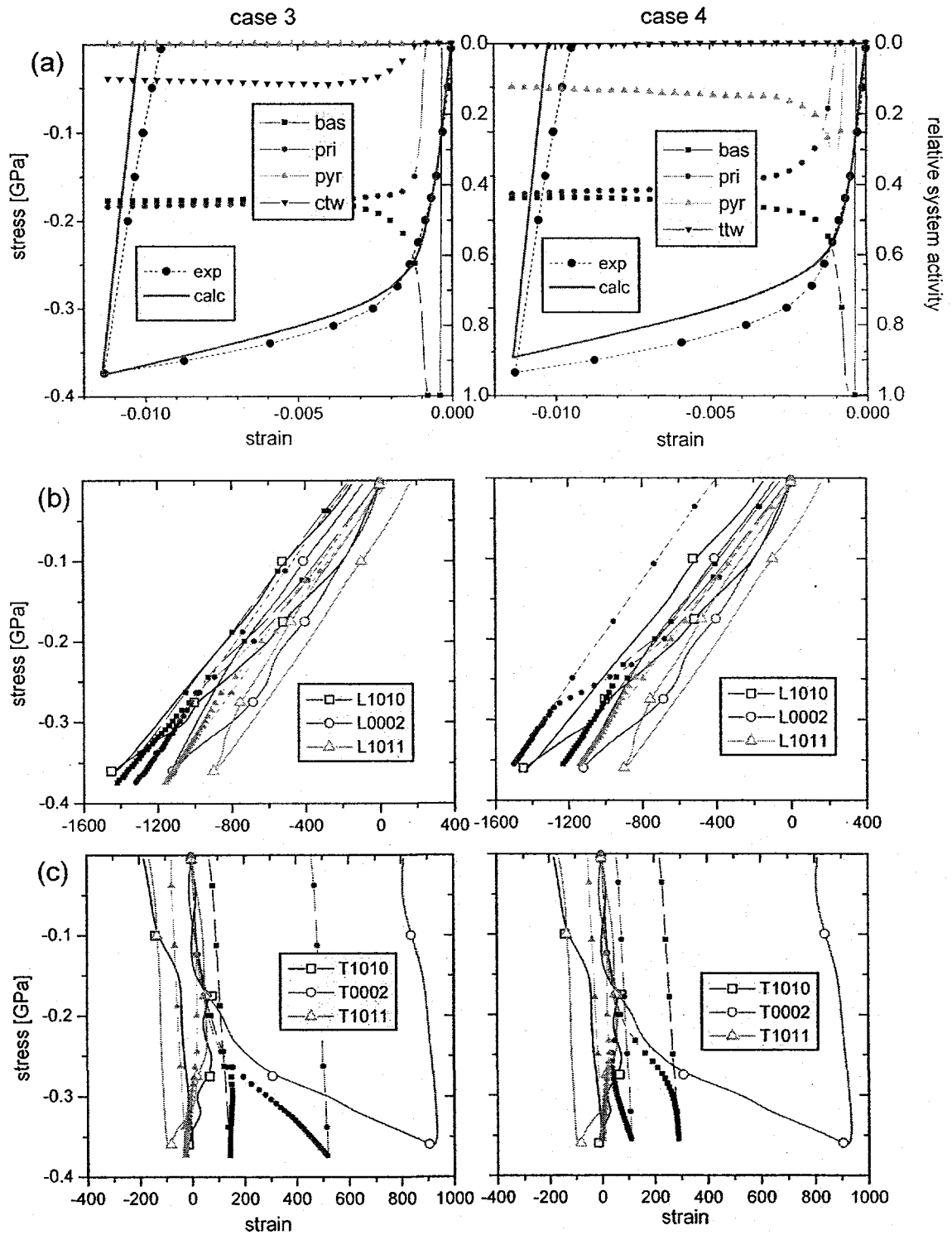
The Lujan Center, Los Alamos Neutron Science Center (LANSCE) at Los Alamos National Laboratory is a national user facility funded by the United States Department of Energy, Office of Basic Energy Science and Defense Programs. This work was supported in part by DOE contract W-7405-ENG-36.

REFERENCES

1. Cheskis HP, Heckel RW, in 'Metal Matrix Composites', ASTM STP 438, American Society for Testing and Materials 1 (1968) 76-91
2. Krawitz AD, Journal of Metals 32 (1980) 72-92
3. Noyan IC, Cohen JB, 'Residual Stress - Measurement by Diffraction and Interpretation' New York, Springer-Verlag (1987)
4. Clausen B, Lorentzen T, Bourke MAM, Daymond MR, Mats Sc and Engng A259 (1999) 17-24
5. Tomé CN, Christodoulou N, Turner PA, Miller M, Woo CH, Root JH, Holden TM, J Nucl Mater 227 (1996) 237-250
6. Pang JWL, Holden TM, Turner PA, Mason TE, Acta Mater 47 (1999) 373-383
7. Turner PA, Christodoulou N, Tomé CN, Int J Plasticity 11 (1995) 251-265
8. Bourke MAM, Goldstone JA, Holden TM, in 'Measurement of Residual and Applied Stress Using Neutron Diffraction' Hutchings MT and Krawitz AD, Eds., Kluwer Academic Publishers. NATO ASI Series E No 216 (1992) 369-382
9. Bourke MAM, Goldstone JA, Shi N, Allison JE, Stout MG, Lawson AC, Scripta Mater 29 (1993) 771-776
10. Webster D, London GJ, Ed. 'Beryllium Science and Technology, Vol. 1'. New York, Plenum Press (1979)



Figures 1 and 2: (a) Measured and predicted stress-strain response during compression of the Be sample. Also shown are the relative contributions of each deformation mode to deformation. (b) Experimental (open symbols) and predicted (full symbols) evolution of strain in longitudinal crystallographic planes. (c) Same as (b) for transverse planes.



Figures 3 and 4: (a) Measured and predicted stress-strain response during compression of the Be sample. Also shown are the relative contributions of each deformation mode to deformation. (b) Experimental (open symbols) and predicted (full symbols) evolution of strain in longitudinal crystallographic planes. (c) Same as (b) for transverse planes.